Immediate Reduction of Cytochrome *c* by Photoexcited NADH: Reaction Mechanism As Revealed by Flow–Flash and Rapid-Scan Studies†

Yutaka Orii

Department of Public Health, Faculty of Medicine, Kyoto University, Kyoto 606, Japan

Received April 14, 1993; Revised Manuscript Received August 23, 1993®

ABSTRACT: Upon exposure of an aqueous solution of NADH and cytochrome *c* to a laser pulse at 355 nm under anaerobic conditions, cytochrome *c* is reduced within 1–2 ms to a maximal extent of 90%. The reduction proceeds in two phases: rapid reduction by hydrated electrons followed by bimolecular electron transfer from the NAD· radical to ferric cytochrome *c*. In addition, a third reduction phase emerges in the presence of an appropriate concentration of molecular oxygen, where the superoxide anion is a reductant. As the oxygen concentration approaches 20% saturation, the cytochrome *c* reduction by NAD· is abolished first and then the reduction by hydrated electrons, since molecular oxygen competes with cytochrome *c* for NAD· and hydrated electrons. At 20% oxygen, cytochrome *c* is reduced almost exclusively by the superoxide anion, but the amount reduced on a single laser pulse is only one-fourth that reduced under anaerobic conditions. The second-order rate constants for the reduction of cytochrome *c* at pH 7.4 and 20 °C by NAD· and the superoxide anion are 2.0×10^9 and 4.0×10^6 M^{-1} s^{-1}, respectively.

Cytochrome *c* is a water-soluble hemoprotein and a ubiquitous electron carrier in a wide variety of photosynthetic and respiratory systems. In the respiratory chain, cytochrome *c* accepts electrons from complex III and transfers them to complex IV, cytochrome *c* oxidase, which catalyzes the reduction of molecular oxygen to water and transforms the redox energy into the proton motive force (Babcock & Wikström, 1992). I have proposed previously that the interaction between cytochrome *c* and oxidase, through the exchange of an electron, modulates the intramolecular electron transfer between the metal centers in the oxidase, and this problem remains to be explored further (Orii, 1988a). One of the difficulties in pursuing this problem is the rapidity with which the electron transfer from ferrocytochrome *c* to cytochrome *c* oxidase proceeds, and a considerable portion of the reaction is lost if it is initiated by mixing the two reactants in a stopped-flow apparatus. Therefore, *in situ* generation of ferrocytochrome *c* in a sub-millisecond time range by suitable means is required to follow spectrophotometrically the whole process of the electron transfer.

Photosensitized reduction of cytochrome *c* in the presence of flavins and EDTA[1] under anaerobic conditions is suitable for that purpose and has been studied extensively (Cusanovich & Tollin, 1980; Meyer et al., 1986; Tollin & Hazzard, 1991; Hazzard et al., 1991; Pan et al., 1991). In this system, the triplet flavin takes an electron from EDTA to yield the semiquinone radical, which in turn reduces cytochrome *c*. Alternatively, a photoreduction system consisting of uroporphyrin and NADH has been used to provide ferrocytochrome *c*. Here, the uroporphyrin triplet state formed by a laser pulse transfers an electron directly to ferricytochrome *c* (Cho et al., 1986; Zhou et al., 1990), but the uroporphyrin π-cation radical thus generated immediately oxidizes the reduced cytochrome. To prevent this reoxidation, NADH is obligatory since it reacts with the π-cation radical more rapidly than ferrocytochrome *c* (Larsen et al., 1992). These two techniques are very useful to study the electron transfer from ferrocytochrome *c* to cytochrome *c* oxidase, to determine the rate constant, and to identify the initial electron acceptor site on the oxidase molecule (Hazzard et al., 1991, 1992; Pan et al., 1991; Larsen et al., 1992). However, the photosensitizers employed so far have absorptions in the Soret and visible regions, so that sometimes the spectral analyses are rendered cumbersome because of spectral overlap with other redox components. A survey of the optically transparent system in this wavelength range is thus prompted.

Czochralska and Lindqvist have reported that, upon irradiation of a deaerated aqueous solution of NADH (pH 10) by a laser pulse at 353 nm of high energy, NADH ejects a hydrated electron, e^-_{aq}, and yields the NAD· radical according to the following reaction scheme (Czochralska & Lindqvist, 1983):

$$\mathrm{NADH} \xrightarrow{h\nu} {}^1\mathrm{NADH} \xrightarrow{h\nu} {}^{\bullet}\mathrm{NADH}^+ + e^-_{aq} \qquad (1)$$

$$^{\bullet}\mathrm{NADH}^+ \xrightarrow{k_2 = 3.5 \times 10^6\ s^{-1}} \mathrm{NAD}^{\bullet} + \mathrm{H}^+ \qquad (2)$$

The initial reaction is assumed to be a two-photon event, and ^{1}NADH is the NADH lowest excited singlet state. Both e^-_{aq} and NAD· are strong reductants since their redox potentials are as low as –2.9 (Buxston et al., 1988) and –0.92 to –0.94 V (Anderson, 1980; Farrington et al., 1980), respectively. Yamazaki and Yokata have proposed previously that NAD· is generated during turnover of horseradish peroxidase in the presence of NADH and a low level of hydrogen peroxide and that this radical reduces molecular oxygen as well as the hemoproteins in the oxidized state (Yamazaki & Yokota, 1967). Therefore, it would be possible to produce ferrocytochrome *c* simply by photoexciting a mixture of NADH and cytochrome *c* if it were not for unfavorable reoxidation of the reduced cytochrome. In the present study, I have observed that indeed the irradiation of a mixture of NADH and cytochrome *c* by the 355-nm laser pulse of 4–6 ns duration efficiently yields ferrocytochrome *c* within 1–2 ms under anaerobic conditions. Furthermore, it has been demonstrated

† This work was supported in part by a research grant from the Fujiwara Foundation of Kyoto University and by a Grant-in-Aid for Scientific Research on Priority Areas of "Cellular Energy" (Grant No. 04266105) from the Ministry of Education, Science and Culture, Japan.

® Abstract published in *Advance ACS Abstracts*, October 15, 1993.

[1] Abbreviations: EDTA, ethylenediaminetetraacetic acid; SOD, superoxide dismutase; e^-_{aq}, hydrated electron.

0006-2960/93/0432-11910$04.00/0

that ferrocytochrome *c* is generated in this time range even in the presence of micromolar levels of molecular oxygen. Previous studies (Cusanovich & Tollin, 1980; Meyer et al., 1986; Tollin & Hazzard, 1991; Hazzard et al., 1991; Pan et al., 1991; Cho et al., 1986; Zhou et al., 1990) have been confined only to the anaerobic reduction. Cytochrome *c* oxidase requires oxygen for the reaction to proceed, so that the aerobic generation of ferrocytochrome *c* is expected to extend the capability of the transient kinetic approach to the reaction mechanism. As a part of a series of studies for that purpose, the present study is focused on establishing the reaction mechanism of the photochemical reduction of cytochrome *c* in the presence of varying concentrations of oxygen.

EXPERIMENTAL PROCEDURES

Materials. Horse heart cytochrome *c* (type III) and bovine erythrocyte superoxide dismutase were obtained from Sigma, and NADH was from Oriental Yeast Co., Ltd. These were used without further purification. Reduction of cytochrome *c* and oxidation of NADH were quantified spectrophotometrically on the basis of the absorbance coefficient differences of $\Delta\epsilon_{mM,550nm}$ = 18.5 (reduced – oxidized) and $\Delta\epsilon_{mM,340nm}$ = 6.22 (reduced – oxidized), respectively. All solutions were made in 50 mM sodium phosphate buffer (pH 7.4), and kinetic measurements were carried out at 20 °C.

Flow–Flash Apparatus. The flow–flash apparatus used in previous studies (Orii, 1984, 1988a,b; Orii et al., 1991) was modified to improve the handling of air-sensitive materials. The reservoirs for sample solutions are made of a heavy-walled quartz tubing (i.d. = 9.8 mm), and the bottom ends are cemented to a ceramic base with a small hole drilled at the center of each for an outlet. The driving syringes are fit to an adjacent ceramic block, which also houses the mixing chamber, the observation cell, and the ball valves. All connections, where applicable, are cemented for air-tightness. The sample solutions are transferred from the reservoirs to the driving syringes through stainless steel tubings (i.d. = 0.8 mm) which connect the two ceramic units *via* ports consisting of Swagelok joints (Swagelok Co., Ltd.). The low ends of the upright driving syringes are covered by a casing made of an aluminum block, and the piston rods move through the bottom holes held by "O" rings. The casing has the inlet and outlet tubings to allow passage of pressurized nitrogen gas. The pull and push of the syringe plungers are driven by the pneumatic actuator, which is operated by pressurized nitrogen gas according to the signals from the controller, and they transfer the sample solutions from the reservoirs to the syringes and from the syringes to the observation cell through the mixing chamber, respectively.

The sample solutions in the reservoirs are bubbled with nitrogen gas, which is conducted by a tubing inserted through the stopper. The stopper also has a gas outlet, allowing the escape of gas and at the same time preventing any back-diffusion of air oxygen. When the sample volume was 4 mL, bubbling was continued for 15 min at a flow rate of less than 30 mL/min. Then the tip of the tubing was lifted above the solution surface, and the gas flushing was continued throughout the experiment. Usually the reactants are concentrated by around 5%, so that the concentrations of the reactants are expressed conventionally for the solutions before deaeration. When necessary, however, the exact concentrations were determined on the basis of the spectral data for a sample solution in the observation cell. By using nitrogen gas as supplied (99.99999%, Teisan Co., Ltd.), the oxygen concentration level attained was much below micromolar since deoxymyoglobin remained unchanged in a parallel experiment. A mixture of nitrogen and oxygen was prepared by the oxygen pump (Toray Co., Ltd., SEP-104) and used to equilibrate the sample solutions in the same way as described above.

When the piston of the pneumatic actuator strikes the stopper after having delivered the sample solutions to the observation cell through the mixing chamber, it triggers the delay circuit that controls the timing of the data acqusition and the laser flash firing. With this unit, it is possible to start the data acquisition and the laser firing at the same time after the mixture stands in the observation cell for a preset delay time, for example, or to delay the laser flash after the initiation of data collection. The laser firing can be isolated from the stopped-flow process. Thus, the reaction mixture in the observation cell can be exposed to a number of laser flashes. In the flow–flash measurements, the photochemical reaction was initiated, unless otherwise described, upon laser flash photolysis of the reaction mixture in the observation cell 10 s after the mixing of the two solutions.

Laser Photolysis. A Q-switched Nd:YAG laser (Continnum, Surelite 10) was used to photoexcite a sample solution in the observation cell of the flow–flash apparatus. Throughout the present study, the third harmonic at 355 nm was used. The total output energy was 40 mJ in a pulse of 4–6-ns duration. The beam spot was transformed into an ellipsoid by using a cylindrical lens and allowed to fall on the quartz window (2 × 10 mm) of the observation cell. The incident energy was at least 10 mJ.

Double Flash and Rapid Scan. A new apparatus was constructed, starting from the original type (Orii, 1984). In this case, a third delay circuit is incorporated: a portion of the laser pulse for photolysis is sensed by a photodiode, which generates a signal to trigger the delay unit for firing a xenon flash lamp (1-μs pulse width, Hamamatsu Photonics, L-4633) for recording the spectrum. This delay unit has a time resolution of 1 μs. A pulse of the xenon flash falls on a bundle of optical fibers, which is branched into two parts at the other end. One is guided to the observation cell and the transmitted light enters the entrance slit of the spectrophotometer, which is equipped with a detector consisting of a double-deck photodiode array (Hamamatsu Photonics, S4801-512Q). The other is guided through a "dummy" cell to the same spectrophotometer. Both sample and reference beams, after having been dispersed, fall on each deck of the diode array. With the incorporation of this technique to compensate for the fluctuation in the light intensity of every xenon flash, the reproducibility of the recorded spectra increased significantly.

Transient Spectrophotometry. The absorbance change at a single wavelength following photolysis of a sample solution in the flow–flash apparatus was followed on the time scale from nanoseconds to milliseconds. The optical system consists of two spectrophotometers with the observation cell in between, and optical fibers made of quartz are used for optical coupling. The first spectrophotometer is equipped with a 150-W xenon lamp as a light source, and the second is equipped with a photomultiplier (Hamamatsu Photonics, R2949). For measurements in sub-microsecond time ranges, a suitable band-pass filter replaced the primary spectrophotometer. The output signal before photolysis is brought to zero by applying an appropriate offset voltage, V_o, and a deviation therefrom following photolysis, ΔV, is fed to a digital oscilloscope (Hewlett-Packard, 54504A). A pulse signal from Surelite 10 triggers recording. Traces from a number of measurements are accumulated on the oscilloscope, and the averaged trace is transferred to a personal computer (NEC, PC98DX2) *via*

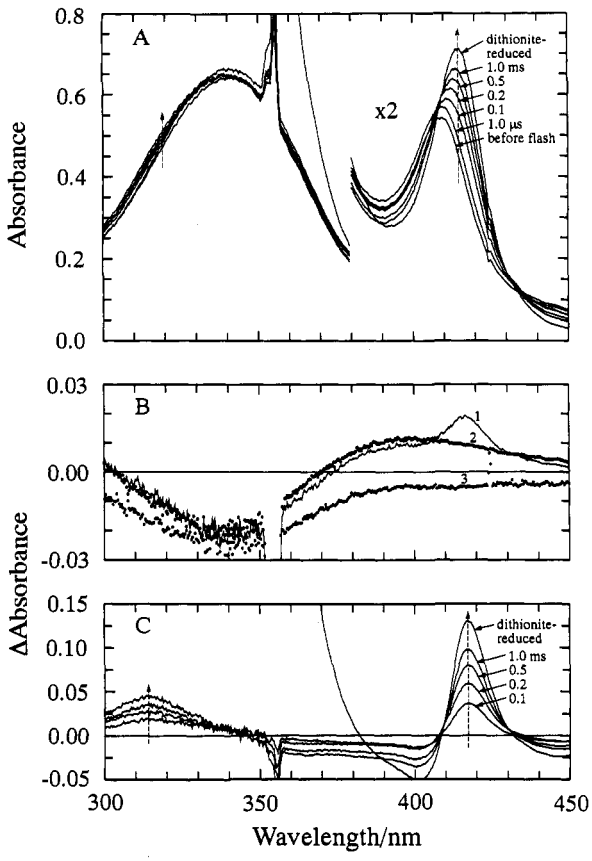

FIGURE 1: Reduction of cytochrome *c* by photoexcited NADH under anaerobic conditions. Deaerated solutions of cytochrome *c* and NADH in 50 mM sodium phosphate buffer (pH 7.4) were mixed in the flow–flash apparatus at 20 °C to give final concentrations of 2.94 and 125 μM, respectively (by calculation). After the solution stood for 10 s, the 355-nm laser pulse was fired to initiate the reaction, followed by a small xenon flash. The measurements were repeated with the refreshed reaction mixtures by changing the laser-to-xenon delay time as indicated in the figure (A). The spectrum before the laser flash and that after dithionite reduction are included for comparison. (B) The 1-μs spectrum after photolysis was obtained using that before photolysis as reference. Spectrum 1 is the deaerated solution containing cytochrome *c* and NADH, spectrum 2 is the deaerated NADH, and spectrum 3 is the aerated NADH solutions. (C) The difference spectra obtained with the 1-μs spectrum as reference. These are derived from the spectra in panel A. A large spike around 355 nm is due to the laser pulse which is not canceled by a control measurement, and a rising absorbance to shorter wavelengths below 380 nm is due to sodium dithionite.

a GPIB interface. A change in absorbance, ΔA, is calculated according to the following equation:

$$\Delta A = \log\left(\frac{V_o}{V_o + \Delta V}\right) \qquad (3)$$

Further details of the instrumentation will be reported elsewhere.

RESULTS AND DISCUSSION

Figure 1A illustrates the spectral changes of an anaerobic mixture of NADH and cytochrome *c* at pH 7.4 initiated by a 355-nm laser pulse. This also includes the spectrum before photolysis and that after dithionite reduction. The photochemical reduction was completed within 1–2 ms after photolysis, but the spectral changes are not monotonous because the spectrum before photolysis does not pass through the isosbestic point shared by most of the spectra recorded after photolysis. In Figure 1B, a difference spectrum between 1 μs after photolysis *and* before photolysis is shown (spectrum 1). A trough at 340 nm indicates a decrease in NADH and a peak at 418 nm indicates the initial reduction of cytochrome *c*. A small, broad peak centered around 400 nm of this spectrum also appeared even in the absence of cytochrome *c* (spectrum 2), in agreement with the spectral profile of the $NAD^{\cdot}$ radical generated by pulse radiolysis (Land & Swallow, 1968) and laser flash photolysis (Czochralska & Lindqvist, 1983). Under aerobic conditions the 400-nm peak did not appear, although the absorbance at 340 nm decreased to almost the same level as was observed under anaerobic conditions (spectrum 3). In this case $NAD^{\cdot}$ must have been quenched by molecular oxygen, which takes an electron from $NAD^{\cdot}$ to become the superoxide anion. On the basis of the absorbance changes at 340 and 418 nm, it is estimated that 3.5 μM NADH is decreased by a single laser pulse, whereas 0.2 μM cytochrome *c* is reduced within 1 μs. According to eqs 1 and 2, this decrease in NADH corresponds to the generation of 7 μM reducing equivalents. Figure 1C illustrates the time difference spectra obtained with the 1-μs spectrum as reference, and it is calculated that, between 1 μs and 1 ms after photolysis, 2.2 μM cytochrome *c* is reduced further, the total being 2.4 μM. This accounts for 76% of the cytochrome *c* (3.15 μM as determined spectrophotometrically) in the reaction mixture. For reduction of the rest, however, dithionite should be added. Therefore, 34% of 7 μM reducing equivalents is used for the reduction of cytochrome *c*. The fate of the rest of the reducing equivalents is discussed later. The spectral profiles below 410 nm in Figure 1C are clearly different from those depicted in Figure 1B: there is no 340-nm trough, and the absorbance increases at 313 nm instead. The absence of the 340-nm trough indicates that the photoexcitation of NADH ceases within 1 μs, and the 313-nm peak may be ascribed to the δ peak of ferrocytochrome *c*.

Figure 2 shows the effect of a number of laser pulses on the mixture of NADH and cytochrome *c*. Under anaerobic conditions, the initial single pulse reduces about 90% of cytochrome *c* this time, and two pulses are sufficient to reduce 2.6 μM cytochrome *c* almost completely. Under aerobic conditions (20% O_2), however, 20 pulses are necessary for the complete reduction. Addition of SOD to the aerobic reaction mixture appreciably suppresses the cytochrome *c* reduction, but it has no effect on the anaerobic reduction. This result suggests that under aerobic conditions superoxide anion is a major reductant. However, a small extent of cytochrome *c* reduction under the aerobic conditions invariably occurred, even in the presence of SOD. In fact, one laser pulse gives rise to SOD-insensitive reduction of 0.035 μM cytochrome *c* on average, which corresponds to 6.7% of the cytochrome that is reduced aerobically on an initial single pulse. This SOD-insensitive aerobic reduction, as well as the anaerobic reduction, must have been achieved by different mechanisms in which the superoxide anion does not participate. A stepwise decrease in absorbance of the 340-nm peak upon laser flash photolysis of the aerobic samples is in contrast to a smaller absorbance change observed with the anaerobic samples. As estimated above, 66% of the reducing equivalents generated under anaerobic conditions is not used for the reduction of cytochrome *c*, leaving part as $NAD^{\cdot}$ radicals. Therefore, it is likely that $NAD^{\cdot}$ dimerizes to yield a species having an absorption at 340 nm (Land & Swallow, 1968). This will counter the absorbance decrease at 340 nm brought about by a loss of NADH. The dimerization does not occur under aerobic conditions because the formation of the superoxide anion is kinetically much faster.

Figure 3 illustrates the effect of oxygen on the photoreduction of cytochrome *c*. In the absence of oxygen, the absorbance change at 418 nm on the 500-ms time scale (panel A) shows that the reduction is almost instantaneous, but the

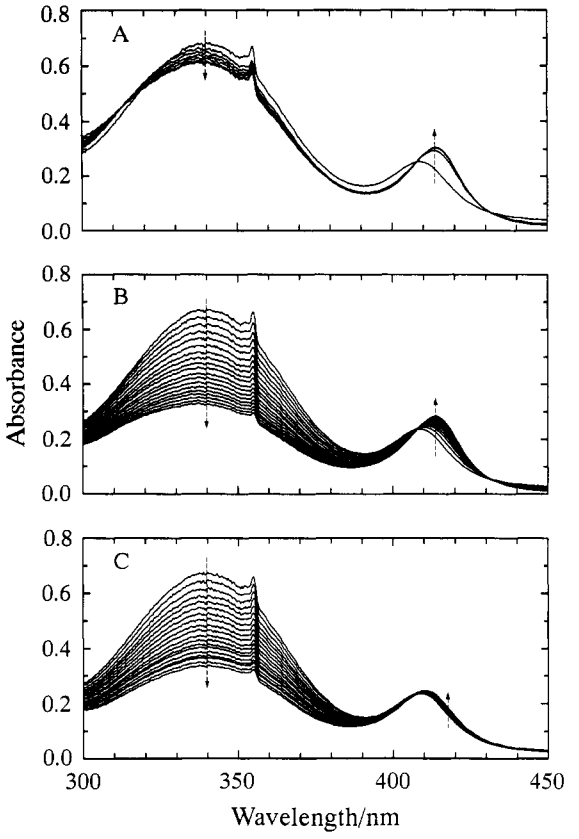

FIGURE 2: Effect of cumulative laser pulses on the reduction of cytochrome c by photoexcited NADH. Either deaerated (A) or aerated (20% O_2) solutions (B and C) of cytochrome c and NADH were mixed on the flow–flash apparatus to final concentrations of 2.61 and 125 μM, respectively (by calculation). All of the spectra were recorded 1 μs after the laser pulse fired every 10 s upon the reaction mixture standing in the observation cell. The reaction mixture in C contained 145 units/mL bovine erythrocyte superoxide dismutase.

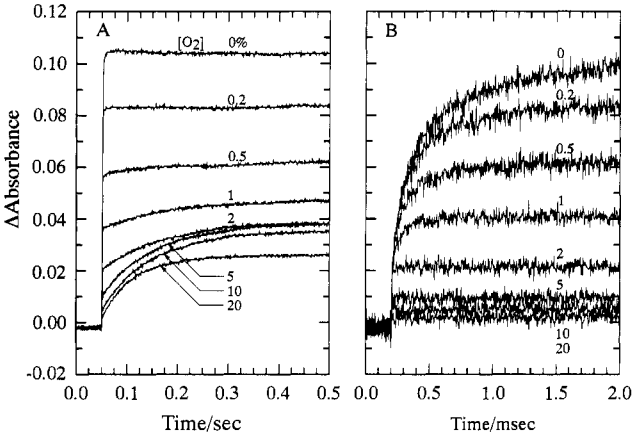

FIGURE 3: Effect of oxygen concentrations on the photoreduction of cytochrome c. Both cytochrome c and NADH solutions in the reservoirs of the flow–flash apparatus were bubbled with gas mixtures of oxygen and nitrogen of varying ratios for 15 min. The photolysis was initiated 10 s after the mixing, and three or five traces at 418 nm were accumulated for A or B, respectively. Panels A and B represent the results of parallel measurements on different time scales. The percent saturations of oxygen are 0, 0.2, 0.5, 1, 2, 5, 10, and 20% from top to bottom.

rapid absorbance increase is resolved into two phases (phases I and II) if the time axis is expanded to the 2-ms scale (panel B). As the oxygen concentration is increased to 0.2 and 0.5% saturation, the maximal reduction level attained decreases, and at 1% a slow absorbance increase following the rapid change becomes apparent on the 500-ms time scale (phase III). At 20% oxygen, phase I is minimal and phase III becomes predominant, although the total amount of cytochrome c reduced is only one-fourth that reduced under anaerobic conditions (panel A). Unique characteristics of phase I deserve further mention. Even under anaerobic conditions phase I was almost negligible when photoreduction was initiated at 1 and 5 ms after mixing of NADH and cytochrome c. When the delay time was extended to 100 ms, phase I became noticeable, but the extent was still lower than one-third that observed with the delay time of 10 s. These results strongly suggest that phase I represents an event occurring in a complex between NADH and cytochrome c, with e^-_{aq} acting as a reductant. The reported value of the rate constant for the reduction of molecular oxygen by e^-_{aq} is 1.88×10^{10} M^{-1} s^{-1} (Willson, 1970). Using this value, the lifetime of the reaction under 2% oxygen, or 28 μM oxygen, is calculated to be 0.13 μs. This value is comparable to the lifetime of 0.15 μs for phase I at 2% oxygen, which was determined in a parallel measurement made on the 2-μs time scale (data not shown), and indicates that cytochrome c complexed with NADH is kinetically as competent as molecular oxygen in reacting with e^-_{aq}. When generated in solution, however, e^-_{aq} may be quenched by oxygen before it encounters cytochrome c. Therefore, it is speculated that only when NADH is juxtaposed to the heme c of a cytochrome c molecule in the complex will the e^-_{aq} ejected by a laser pulse efficiently attack the heme in a "right" place. If only the e^-_{aq} ejected from the NADH complexed to cytochrome c were allowed to reduce the heme c moiety, this reaction would obey first-order kinetics. Thus, the lifetime of 0.15 μs is tentatively converted to the first-order rate constant of 4.6×10^6 s^{-1}.

It is to be noted that at and above 2% oxygen, phase II is suppressed almost completely but phases I and III persist (panel B). In the pulse radiolysis study of NADH, Czochralska and Lindqvist have reported that a species having a peak at 400 nm is ascribed to the NAD· radical being generated by deprotonation of $\cdot NADH^+$ with a rate constant of 3.6×10^6 s^{-1} ($t_{1/2}$ = 0.2 μs) (Czochralska & Lindqvist, 1983). The $NAD^+/NAD\cdot$ couple has a fairly low redox potential of –0.92 to –0.94 V at pH 7 (Anderson, 1980; Farrington et al., 1980) and reduces molecular oxygen with a rate constant of $(1.9–2.0) \times 10^9$ M^{-1} s^{-1} (Willson, 1970; Land & Swallow, 1971). Therefore, the abolishment of phase II strongly suggests that molecular oxygen takes an electron from NAD·, which otherwise will reduce cytochrome c rapidly. The superoxide anion thus produced reduces cytochrome c in phase III. In fact, generation of the superoxide anion under the continuous illumination of NADH or NADPH with ultraviolet light from 290 to 405 nm, as detected by aerobic reduction of cytochrome c, has been reported (Cunningham et al., 1985). The persistence of phase II in the presence of nearly equimolar amounts of oxygen and cytochrome c (0.2 and 0.5% oxygen saturation in Figure 3B) will be ascribed to the competition of these two species for NAD·.

Figure 4 illustrates a kinetic profile of the reduction of cytochrome c by NAD·. The data from 100 μs onward in the top trace in Figure 3B, which represent phase II, were subjected to curve-fitting based on a second-order reaction model. With 2.1 μM ferricytochrome c remaining at the start, the concentration of NAD· at the start and the rate constant were estimated to be 1.3 μM and 2.0×10^9 M^{-1} s^{-1}, respectively. The coincidence of this rate constant with that for the reaction between NAD· and oxygen, $(1.9–2.0) \times 10^9$ M^{-1} s^{-1} (Willson, 1970; Land & Swallow, 1971), supports the possibility of competition between cytochrome c and oxygen for NAD· as described above.

In conclusion, the relevant reactions that explain the photoreduction of cytochrome c observed in the present study

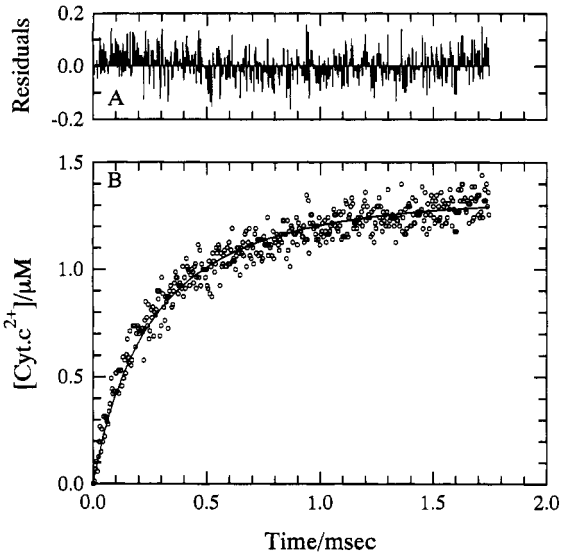

FIGURE 4: Kinetic analysis of phase II reduction. The data point at 100 μs after photolysis in the top trace of Figure 3B was assumed to be the origin for the reduction of cytochrome *c* by NAD, and the absorbance increase thereafter was converted to the concentration of ferrocytochrome *c* spectrophotometrically and subjected to curve-fitting according to the following equation for the second-order reaction: $[c^{2+}] = ([NAD^{\cdot}]_{int} \exp(pkt + q) - [c^{3+}]_{int})/(\exp(pkt + q) - 1)$, where $p = [c^{3+}]_{int} - [NAD^{\cdot}]_{int}$ and $q = \ln([c^{3+}]_{int}/[NAD^{\cdot}]_{int})$. The initial concentration of ferricytochrome *c* in the analysis, $[c^{3+}]_{int}$, was 0.0021 mM. This was estimated by subtracting the concentration of cytochrome *c* reduced during the initial 100 μs from its total concentration in the reaction mixture. The initial concentration of NAD$^{\cdot}$ and the rate constant were treated as unknowns in the fitting. A solid line in B was obtained by calculation with $[NAD^{\cdot}] = 0.0013$ mM and $k = 2.0 \times 10^9$ M^{-1} s^{-1}.

Table I: Rate Constant for Reduction of Cytochrome *c* by the Superoxide Anion

$[O_2]$ in % satn	[cyt c^{3+}]/μM	$[O_2^-]$/μM	$k/10^6$ M^{-1} s^{-1}	r^2
20	2.87	0.541	6.15 ± 0.03	0.996[a]
10	2.77	0.691	4.02 ± 0.02	0.998
5	2.67	0.643	3.84 ± 0.02	0.997
2	2.43	0.425	3.53 ± 0.03	0.994
1	2.12	0.267	4.54 ± 0.06	0.976

[a] Correlation coefficients in the fitting. Experimental conditions are described in the legend to Figure 3. The data from Figure 3A are subjected to curve-fitting according to the model of a second-order reaction. The initial concentrations of ferricytochrome *c* in phase III are determined on the basis of the trace data and used as defined in the fitting. The concentrations of superoxide anion and the second-order rate constant are treated as unknowns and derived as described in the legend to Figure 4.

are summarized as follows:

$$e^-_{aq} + \text{cyt } c^{3+} \xrightarrow{k_4 = 4.6 \times 10^6\ s^{-1}} \text{cyt } c^{2+} \quad \text{(4, phase I)}$$

$$NAD^{\cdot} + \text{cyt } c^{3+} \xrightarrow{k_5 = 2.0 \times 10^9\ M^{-1}\ s^{-1}} NAD^+ + \text{cyt } c^{2+} \quad \text{(5, phase II)}$$

$$NAD^{\cdot} + O_2 \xrightarrow{k_6 = 1.9 \times 10^9\ M^{-1}\ s^{-1}} NAD^+ + {}^{\cdot}O \quad \text{(6, ref 21)}$$

$${}^{\cdot}O_2^- + \text{cyt } c^{3+} \xrightarrow{k_7 = 4.0 \times 10^6\ M^{-1}\ s^{-1}} O_2 + \text{cyt } c^{2+} \quad \text{(7, phase III)}$$

The rate constants for the reduction of cytochrome *c* by the superoxide anion in phase III are derived from the data in Figure 3A and summarized in Table I. At 1, 2, 5, and 10% oxygen saturations, the estimated second-order rate constants are quite similar, giving an average value of 4.0×10^6 M^{-1} s^{-1}. It is to be noted that this is $^1/_{500}$ that for the reduction by NAD. The rate constant determined at 20% oxygen saturation is somehow higher than the rest, and the cause of this deviation remains to be investigated. These results are consistent with the previous finding that the photoexcitation of NADH with the high-intensity 353-nm laser pulse ejects hydrated electrons and generates NAD$^{\cdot}$ radicals as well *via* deprotonation of $^{\cdot}$NADH$^+$ (Czochralska & Lindqvist, 1983). It is to be noted that the reactivity of NAD$^{\cdot}$ as a reductant is as high as that of 5-deazariboflavin semiquinone in terms of the second-order rate constant (2.0×10^9 M^{-1} s^{-1} *versus* ($2–3$) $\times 10^9$ M^{-1} s^{-1}) for the reduction of *c*-type cytochromes (Hazzard et al., 1991; Tollin & Hazzard, 1991). Furthermore, NAD$^{\cdot}$ has some advantages, such that it is derived from a physiological substance, is practically colorless above 380 nm, and is readily available. NADPH also behaves similar to NADH, as will be reported elsewhere.

Therefore, the present technique can be applied to a wide range of redox components to reveal intricate mechanisms of the biological electron-transfer processes, and kinetic analyses of the initial steps from ferrocytochrome *c* thus generated to cytochrome *c* oxidase are under way.

ACKNOWLEDGMENT

I am grateful to Dr. Toshihiko Nagamura of Unisoku Co., Ltd. for his excellent assistance and efforts in constructing the kinetic instruments employed in the present study.

REFERENCES

Anderson, R. F. (1980) *Biochim. Biophys. Acta 590*, 277–281.
Babcock, G. T., & Wikström, M. (1992) *Nature 356*, 301–309.
Buxston, G. V., Greenstock, C. L., Helman, W. P., & Ross, A. B. (1988) *J. Phys. Chem. Ref. Data 17*, 513–531.
Cho, K. C., Che, C. M., Ng, K. M., & Choy, C. L. (1986) *J. Am. Chem. Soc. 108*, 2814–2818.
Cunningham, M. L., Johnson, J. S., Giovanazzi, S. M., & Peak, M. J. (1985) *Photochem. Photobiol. 42*, 125–128.
Cusanovich, M. A., & Tollin, G. (1980) *Biochemistry 19*, 3343–3347.
Czochralska, B., & Lindqvist, L. (1983) *Chem. Phys. Lett. 101*, 297–299.
Farrington, J. A., Land, E. J., & Swallow, A. J. (1980) *Biochim. Biophys. Acta 590*, 273–276.
Hazzard, J. T., Rong, S., & Tollin, G. (1991) *Biochemistry 30*, 213–222.
Hazzard, J. T., Mauk, A. G., & Tollin, G. (1992) *Arch. Biochem. Biophys. 298*, 91–95.
Land, E. J., & Swallow, A. J. (1968) *Biochim. Biophys. Acta 162*, 327–337.
Land, E. J., & Swallow, A. J. (1971) *Biochim. Biophys. Acta 234*, 34–42.
Larsen, R. W., Winkler, J. R., & Chan, S. I. (1992) *J. Phys. Chem. 96*, 8023–8027.
Meyer, T. E., Bartsch, R. G., Cheddar, G., Getzoff, E. D., Cusanovich, M. A., & Tollin, G. (1986) *Biochemistry 25*, 1383–1390.
Orii, Y. (1984) *J. Biol. Chem. 259*, 7187–7190.
Orii, Y. (1988a) *Ann. N.Y. Acad. Sci. 550*, 105–117.
Orii, Y. (1988b) *Chem. Scr. 28A*, 63–69.
Orii, Y., Yumoto, I., Fukumori, Y., & Yamanaka, T. (1991) *J. Biol. Chem. 266*, 14310–14316.
Pan, L.-P., Hazzard, J. T., Lin, J., Tollin, G., & Chan, S. I. (1991) *J. Am. Chem. Soc. 113*, 5908–5910.
Tollin, G., & Hazzard, J. T. (1991) *Arch. Biochem. Biophys. 287*, 1–7.
Willson, R. L. (1970) *Chem. Commun. 1970*, 1005.
Yamazaki, I., & Yokota, K. (1967) *Biochim. Biophys. Acta 132*, 310–320.
Zhou, J. S., Granada, E. S. V., Leontis, N. B., & Rodgers, M. A. J. (1990) *J. Am. Chem. Soc. 112*, 5074–5080.